HHS Public Access

Author manuscript

J Invest Dermatol. Author manuscript; available in PMC 2022 January 01.

Published in final edited form as:

J Invest Dermatol. 2021 January ; 141(1): 142–151.e6. doi:10.1016/j.jid.2020.05.080.

Integrin α3β1 on tumor keratinocytes is essential to maintain tumor growth and promotes a tumor-supportive keratinocyte secretome.

Whitney M. Longmate[1], **Scott Varney**[1], **Derek Power**[1], **Rakshitha Pandulal Miskin**[2], **Karl E. Anderson**[1], **Lori DeFreest**[1], **Livingston Van De Water**[1,2], **C. Michael DiPersio**[1,2]

[1]Department of Surgery, Cancer Cell Biology, Albany Medical College, Albany, NY 12208, USA

[2]Department of Regenerative and Cancer Cell Biology, Albany Medical College, Albany, NY 12208, USA

Abstract

Development of integrin-targeted cancer therapies is hindered by incomplete understanding of integrin function in tumor cells and the tumor microenvironment. Previous studies showed that mice with epidermis-specific deletion of the α3 integrin subunit fail to form skin tumors during two-step chemical tumorigenesis, indicating a pro-tumorigenic role for integrin α3β1. Here we generated mice with tamoxifen-inducible, epidermis-specific α3 knockout to determine the role of α3β1 in the maintenance of established tumor cells and/or the associated stroma. Genetic ablation of α3 in established skin tumors caused their rapid regression, indicating that α3β1 is essential to maintain tumor growth. Interestingly, while reduced proliferation and increased apoptosis were observed in α3β1-deficient tumor cells, these changes followed a robust increase in stromal apoptosis. Furthermore, macrophages and fibulin-2 levels were reduced in stroma following α3 deletion from tumor cells. Mass spectrometric analysis of conditioned medium from immortalized keratinocytes showed that α3β1 regulates a substantial fraction of the keratinocyte secretome, including fibulin-2 and macrophage colony-stimulating factor 1; RNA *in situ* hybridization showed that expression of these two genes was reduced in tumor keratinocytes *in vivo*. Our findings identify α3β1 as a regulator of the keratinocyte secretome and skin tumor microenvironment, and as a potential therapeutic target.

Author for correspondence: C. Michael DiPersio, Ph.D., Current Address: Albany Medical College, Mail Code 165, Room MR-424, 47 New Scotland Avenue, Albany, NY 12208-3479, dipersm@mail.amc.edu, phone: (518) 262-5916, fax: (518) 262-5669.

AUTHOR CONTRIBUTIONS

Conceptualization: WML, LV, CMD; Data Curation: WML, SV; Formal Analysis: WML, SV, DP, KEA; Funding Acquisition: LV, CMD; Investigation: WML, SV, DP, RPM, KEA, LD; Methodology: WML, SV, DP, LV, CMD; Project Administration: LV, CMD; Resources: LV, CMD; Software: SV, DP; Supervision: WML, LV, CMD; Validation: WML, SV, DP, RPM, KEA; Visualization: WML, CMD; Writing - Original Draft Preparation: WML, CMD; Writing - Review and Editing: WML, SV, LV, CMD.

DATA AVAILABILITY

Datasets related to this article can be found at the ProteomeXchange Consortium (http://www.ebi.ac.ul/pride) via the PRIDE (Perez-Riverol et al., 2019) partner repository (dataset identifier PXD018425).

CONFLICT OF INTEREST

The authors declare no potential conflicts of interest.

INTRODUCTION

As the major cell surface receptors for the extracellular matrix (ECM), integrins are well-known to regulate adhesion and migration (Hynes, 2002). However, numerous studies have solidified additional roles for integrins that extend beyond such regulation, identifying them as important mediators of communication between the cell and tissue microenvironment (Hynes, 2002). Indeed, integrins have critical roles in the dynamic and reciprocal interactions that occur between tumor cells and the tumor microenvironment (TME) that drive tumor growth and progression (Cooper and Giancotti, 2019, Hamidi and Ivaska, 2018). Previous studies using both wound healing and tumor models, have identified important roles for the laminin-binding integrin, α3β1, in normal and pathological tissue remodeling, as reviewed (Longmate et al., 2017, Longmate et al., 2014). In particular, we previously identified important roles for α3β1 in the regulation of paracrine crosstalk from keratinocytes to endothelial cells that promotes wound angiogenesis (Mitchell et al., 2009), and from keratinocytes to fibroblasts that controls their differentiation state (Zheng et al., 2019). However, roles for integrins in regulation of the TME remain underexplored.

It is now understood that communication between tumor cells and stromal cells promotes a TME that supports ECM remodeling, tumor cell proliferation, and angiogenesis (Hanahan and Weinberg, 2011, Joyce and Pollard, 2009, Marcucci et al., 2014). Much of what we know about intercellular crosstalk within the TME derives from models of cutaneous squamous cell carcinoma (SCC) (Lim and South, 2014) and extends to other cancers (Abel et al., 2009, Ratushny et al., 2012). The two-step skin tumorigenesis model remains one of the best characterized murine models to investigate stepwise cancer development and recapitulates many features of human carcinogenesis (Abel et al., 2009). In this model, a single treatment with DMBA (7,12-dimethylbenz[a]-anthracene) causes “initiation” of keratinocyte stem cells primarily through activation of *Hras1*, followed by “promotion” where repeated treatment over weeks with TPA (12-O-tetradecanoylphorbol-13-acetate) induces benign skin tumors (i.e., papillomas), a proportion of which progress to SCC depending on the genetic background (Abel et al., 2009). In this model, epidermis-specific ablation of α3β1 through Cre-mediated deletion of floxed *Itga3* alleles ($\alpha3^{flx/flx}$) reduces both incidence and size of skin papillomas, demonstrating that this integrin is essential for tumor formation (Longmate et al., 2017, Sachs et al., 2012). However, greatly reduced papilloma formation in these mice precluded investigation of the role that tumor cell α3β1 may play in regulation of the TME and *maintaining* tumor growth. To address this, we generated $\alpha3^{flx/flx}$ mice that carry a keratin-14 (K14) promoter-driven, tamoxifen-inducible Cre transgene (Tg(KRT14-cre/ERT)), wherein topical skin treatment with tamoxifen causes deletion of floxed genes in the epidermis and hair follicles (Vasioukhin et al., 1999), allowing us to assess the impact of ablating epidermal α3β1 on growing tumors. Hereafter, these mice are referred to as K14CreERT:$\alpha3^{flx/flx}$.

Strikingly, tumors in which epidermal α3 was deleted regressed rapidly, and tumor cells displayed both reduced proliferation and enhanced apoptosis. Interestingly, a marked increase in apoptosis was detected within the stromal compartment before comparable changes were detected in tumor cells, indicating that the impact of α3β1 ablation is not restricted to cell-autonomous effects, but likely includes paracrine effects on stromal cells

and/or alterations of the ECM. Indeed, we observed a reduced number of macrophages and reduced fibulin-2 deposition into the stroma of α3β1-deficient tumors. Mass spectrometry (MS) of conditioned medium from immortalized keratinocytes revealed that a substantial portion of the secretome is regulated by α3β1, including many proteins associated with matrix remodeling or paracrine stimulation of macrophages or other stromal cells. In addition, Gene Set Enrichment Analysis (GSEA) revealed that the α3β1-dependent keratinocyte secretome was enriched in human SCC with high *ITGA3* expression. RNA *in situ* hybridization (ISH) demonstrated that expression of the genes for two of these proteins, fibulin-2 and macrophage colony-stimulating factor 1 (CSF1), was reduced in the tumor cells of skin tumors. Our results demonstrate that α3β1 is essential to maintain tumor growth and regulate the keratinocyte secretome, suggesting that α3β1-dependent paracrine signals from tumor keratinocytes contribute to a tumor-supportive TME.

RESULTS

Deletion of integrin α3β1 from epidermal cells of established skin tumors leads to tumor regression

K14CreERT:$\alpha3^{flx/flx}$ mice were subjected to DMBA/TPA two-step tumorigenesis model wherein *Itga3* mRNA is increased in tumors compared with normal skin (Fig. S1). Well after tumors had formed (19 weeks of age, Fig. 1a), mice were treated with topical application of (Z)-4-hydroxytamoxifen (4OHT), or vehicle as control. Immunostaining showed that α3 expression was reduced substantially within 3 days of 4OHT treatment and was undetectable by 7 days post-treatment (shown in Fig. 1f). Strikingly, loss of α3β1 from 4OHT-treated tumors caused dramatically reduced tumor volume (Fig. 1a) and number (Fig. 1b,c) post-treatment, while papillomas of control mice continued to grow, indicating that α3β1 is essential to *maintain* tumor growth. Histologically, 4OHT-treated tumors, while smaller, appeared structurally similar to control tumors and displayed features characteristic of cutaneous papillomas, including hyperplastic epidermal tumor cell nests that often contained keratinized cores and were interdigitated by a vascularized stroma (Fig. 1d; all images are from entirely within a tumor).

The most remarkable reduction in tumor volume occurred in the initial 2-week period following 4OHT treatment of K14CreERT:$\alpha3^{flx/flx}$ mice (Fig. 1a); therefore, we more closely assessed this regression period. Skin tumors were induced as before, then measured and collected every 3–4 days for 2 weeks following 4OHT treatment. We observed a trend toward reduced tumor volume at treatment day 3, and a significant reduction in volume at treatment day 7 (Fig. 1e). Immunofluorescence showed that epidermal α3 was substantially reduced by 3 days after 4OHT-treatment and nearly undetectable by 7 days (Fig. 1f). Importantly, 4OHT treatment of K14CreERT:$\alpha3^{+/+}$ mice (i.e., lacking $\alpha3^{flx/flx}$ alleles and expressing α3β1) did not significantly alter papilloma volume compared with control at any timepoint (Fig. S2). These results demonstrate that α3β1 is required in tumor keratinocytes to maintain tumor growth.

Regression of α3β1-deficient papillomas is accompanied by reduced proliferation of tumor cells and increased apoptosis of both stromal and tumor cells

We next investigated the underlying cause of tumor regression upon deletion of α3β1 from tumor cells. Our previous work showed that α3β1 promotes the secretion of factors by keratinocytes and breast cancer cells that stimulate endothelial cell migration, identifying a pro-angiogenic role for α3β1 (Longmate et al., 2017, Mitchell et al., 2010, Mitchell et al., 2009). However, we did not detect changes in blood vessel density (Fig. S3a,b) or relative stromal area (Fig. S3c) in regressing tumors.

Immunostaining for Ki67 revealed that proliferating tumor cells were located along the tumor-stroma boundary (Fig. 2a). This staining was significantly reduced in α3β1-deficient papillomas by 7 days post-4OHT treatment (Fig. 2a,b), coinciding with reduced tumor volume (e.g., Fig. 1e).

TUNEL-staining during regression of α3β1-deficient tumors (Fig. 2c) revealed a statistically significant increase in apoptosis, compared with control tumors, that was detected by 7 days post-4OHT treatment in both the tumor cell compartment (Fig. 2d, “tumor epithelium”) and the stromal compartment (Fig. 2e, “tumor stroma”). However, quantification of TUNEL+ cells within each compartment over the time course of tumor regression (i.e., from the same sections at each time point) revealed a difference in the timing of peak apoptotic activity between these compartments. Indeed, TUNEL-staining peaked (~10-fold > control) in the stroma of α3β1-deficient papillomas at treatment day 7, followed by a decline that presumably reflects clearance of apoptotic cells (Fig. 2e). In contrast, peak apoptotic activity (~10-fold > control) occurred later in the tumor cell compartment, at treatment day 14 (Fig. 2d). Thus, ablating α3β1 in tumor cells altered stromal apoptosis within the TME, and peak apoptotic response in the stroma preceded that in epithelial tumor cells.

To directly address cell-autonomous effects of α3β1 ablation on proliferation or apoptosis, we exploited a panel of immortalized (IMK) or transformed (TMK) keratinocyte lines that we derived previously from mice that lack (α3−) or express (α3+) α3β1 (Lamar et al., 2008). We detected no α3β1-dependent difference in survival of IMK cells or TMK cells when challenged with serum-free growth conditions (Fig. S4a). Furthermore, we detected no effect of deleting α3β1 on IMK cell proliferation (Fig. S4b), and only a modest (albeit statistically significant) decrease in TMK cell proliferation (Fig. S4c). TMKα3− cells showed a small increase in proliferation when grown in 1:1 co-culture with TMKα3+ cells, compared with when grown alone (Fig. S4d), suggesting that the proliferation difference between TMKα3+ and TMKα3− cells is at least partly due to α3β1-dependent secreted factors. These findings indicate that α3β1-dependent effects on tumor keratinocyte proliferation and survival become prominent in the *in vivo* context of the TME. Consistently, we showed previously that TMKα3+ cells are tumorigenic while TMKα3− cells are not (Lamar et al., 2008).

Integrin α3β1 regulates the keratinocyte secretome

To investigate α3β1 regulation of the keratinocyte secretome, we utilized immortalized mouse keratinocyte (MK) cell lines that we established previously, which either lack α3β1

due to α3-null mutation (MKα3−) or express α3β1 through stable rescue with human α3 (MKα3+) (Iyer et al., 2005). In order to profile the α3β1-dependent MK secretome, serum-free medium was conditioned for 24 hours by MKα3+ or MKα3− cells then analyzed by MS. Of 494 total quantified secreted proteins, 228 (~46%) were at least 50% higher (144 total) or lower (84 total) in the conditioned medium of MKα3+ cells, compared with MKα3− cells. Many of these α3β1-dependent, secreted proteins are ECM proteins, growth factors, proteases/MMPs or their inhibitors, or cytokines with known roles in ECM assembly or paracrine stimulation of stromal cells (a partial list is shown in Table S1). Importantly, some of these proteins were previously identified as α3β1-dependent *in vivo* and/or *in vitro* (Longmate et al., 2018, Longmate et al., 2014, Missan et al., 2014, Mitchell et al., 2009, Zheng et al., 2019), or the corresponding gene was α3β1-dependent in the MK transcriptome (Missan et al., 2014), validating use of MS to profile the α3β1-dependent MK secretome. Gene set enrichment analysis (GSEA) using a gene set corresponding to the α3β1-dependent MK secretome demonstrated that it is enriched in mouse papillomas compared to tumor-free mouse skin (Fig. S5), indicating that the MK secretome is reflective of tumorigenic gene expression programs *in vivo*.

Next, we determined if the α3β1-dependent MK secretome correlates with expression of the α3 subunit gene (i.e., *ITGA3*) in human SCC. We generated a gene set of human homologs of the genes for upregulated proteins in the α3β1-dependent MK secretome (see above), then performed GSEA of RNAseq data from 500 human SCC samples. GSEA revealed that the α3β1-dependent secretome gene set was significantly enriched in the '*ITGA3* high' group, compared with the '*ITGA3* low' group (Fig. 3a). Core enriched genes in the '*ITGA3* high' group (Fig. 3b,c) include: (1) growth factors (e.g., VEGFC, CSF1, CSF2, CSF3); (2) secreted proteases or matrix proteins, some previously shown as α3β1-dependent in MK cells (e.g., BMP-1, MMP-3, MMP-10, MMP-14, laminin γ2) (Longmate et al., 2017, Longmate et al., 2018); (3) the cytokine IL-1α, which we showed mediates keratinocyte-to-fibroblast crosstalk (Zheng et al., 2019). This GSEA validates our MK model to investigate α3β1 regulation of the keratinocyte secretome with potential relevance to human SCC.

Macrophages are reduced during regression of α3β1-deficient tumors

Several α3β1-dependent proteins in the MK secretome have known roles in crosstalk to inflammatory cells, such as tumor-associated macrophages (e.g., CSF1, CSF2, CSF3, CXCL5, IL-1α). A recent study linked αvβ3 integrin expression on tumor cells with accumulation of tumor-associated macrophages in human and mouse tumors (Wettersten et al., 2019). Interestingly, we detected a significant decrease in CD11b-positive leukocytes in α3β1-deficient tumors by 10 days post-4OHT treatment, compared to control tumors (Fig. 4a,b). Moreover, immunostaining for the murine macrophage marker, F4/80, revealed a significant decrease in macrophages by treatment day 10 (Fig. 4c), indicating that macrophages are at least one CD11b-positive population that is decreased in α3β1-deficient tumors. Co-localization of TUNEL-staining with F4/80 staining was increased ~2.5-fold in 7-day 4OHT-treated tumors compared with control tumors (Fig. 4d), although some TUNEL +/F4/80− cells were also detected (Fig. 4e). Thus, increased macrophage apoptosis may contribute to their loss from the stroma of α3β1-deficient tumors, although we cannot rule out additional effects on the recruitment of macrophages or other leukocytes.

Expression of fibulin-2 and CSF1 are reduced in tumor cells of α3β1-deficient tumors

The matricellular protein, fibulin-2, was among the ECM proteins detected in the α3β1-dependent MK secretome (Table S1). This finding is consistent with our previous report that α3β1 promotes the expression of fibulin-2 in immortalized/transformed mouse keratinocytes *in vitro* (Missan et al., 2014) and in murine neonatal skin and adult wounds *in vivo* (Longmate et al., 2014). Roles for fibulin-2 in cancer progression remain unclear and may be context dependent, as it has been described as both a promoter of malignancy and a tumor suppressor (Obaya et al., 2012). We demonstrated previously that suppression of fibulin-2 in transformed keratinocytes reduced their invasiveness (Missan et al., 2014). Interestingly, immunohistology showed reduced fibulin-2 in the stroma of α3β1-deficient tumors by 14 days post-4OHT treatment compared with control tumors (Fig. 5a,b), confirming that its α3β1-dependent expression in the MK secretome (Table S1) reflects its expression pattern in the two-step tumorigenesis model. Since some stromal cells may deposit fibulin-2, we assessed fibulin-2 mRNA expression within the tumor cell compartment using RNAscope ISH of cryosections (Wang et al., 2012). Histological scoring revealed that fibulin-2 mRNA was detected primarily within the tumor cell compartment, and was reduced substantially in α3β1-deficient tumor cells compared with control tumor cells (Fig. 5c), indicating that lower fibulin-2 gene expression in these cells contributes to reduced fibulin-2 deposition into the TME.

As described above, we observed reduced macrophages in 4OHT-treated tumors (Fig. 4). In addition, CSF1, a primary regulator of macrophage differentiation, proliferation and survival (Jones and Ricardo, 2013), was α3β1-dependent in the MK secretome (Table S1) and core-enriched in our GSEA (Fig. 3). Consistently, RNAscope analysis showed that CSF1 mRNA was reduced in α3β1-deficient tumor cells, compared with control tumor cells (Fig. 5d), further linking our MS secretome data to the *in vivo* skin tumorigenesis model.

In summary, α3β1-dependent expression of fibulin-2 and CSF1 within the MK secretome reflects their gene expression within skin tumors, suggesting that integrin α3β1 on tumor keratinocytes regulates the secretion of factors that may confer tumor-supportive properties to the TME (Fig. 5e).

DISCUSSION

Here we report that α3β1 on tumor cells promotes a tumor-supportive TME, likely through secretion of soluble factors that modify the ECM and mediate paracrine crosstalk to stromal cells. Consistently, our past studies established a role for keratinocyte α3β1 in regulating the production of both extracellular proteases and growth factors that stimulate endothelial cells, fibroblasts and potentially other stromal cells (Longmate et al., 2017, Mitchell et al., 2010, Mitchell et al., 2009, Zheng et al., 2019). Moreover, a recent study of epidermolysis bullosa caused by inherited *ITGA3* mutation in humans, showed that absence of keratinocyte α3β1 leads to changes in the extracellular composition of the skin microenvironment (He et al., 2018).

Here we used a model wherein α3 can be deleted specifically in epidermal tumor cells with temporal control, through topical application of tamoxifen, to show that ablation of α3β1

from the tumor cell compartment resulted in rapid tumor regression. During the regression phase following α3 deletion we observed robust stromal apoptosis prior to robust apoptosis within the α3β1-deficient tumor cells, suggesting that changes in the TME contributed to tumor regression, perhaps through loss of stromal cues that maintain tumor cell survival. Consistently, absence of α3β1 from cultured TMK cells did not alter survival upon serum starvation and had only a modest effect on proliferation, indicating that α3β1-dependency requires the *in vivo* context of the TME. Together, our findings suggest that α3β1 on tumor keratinocytes promotes paracrine signals and stromal matrix remodeling that contributes to a tumor-supportive TME (Fig. 5e).

Consistent with our model, MS of the keratinocyte secretome identified α3β1-dependent expression of cytokines, growth factors, proteases, and matrix-associated proteins. Moreover, GSEA revealed that this α3β1-dependent secretome shows concordant differences in human SCC with high vs. low *ITGA3* expression. Since we did not remove exosomes from conditioned media prior to MS analysis, we used the human and animal secretome and subcellular proteome knowledgebase (MetazSecKB) to generate a list of α3β1-dependent secreted proteins (Meinken et al., 2015). However, exosomes have been implicated as important mediators of crosstalk between tumor cells and stromal cells (Yang et al., 2019), so it will be interesting in future studies to determine the extent to which tumor cell α3β1 controls the profile of protein cargo in exosomes.

Our previous work established roles for epithelial α3β1 in paracrine crosstalk to endothelial cells and stimulation of angiogenesis in wound and breast cancer models (Mitchell et al., 2010, Mitchell et al., 2009). Although we did not observe evidence of such a role for α3β1 in skin tumors, our findings do not preclude a pro-angiogenic role for α3β1 during early papilloma growth or for qualitative aspects of blood vessels. Nevertheless, we detected substantial alterations of the TME following deletion of α3 from tumor cells. Firstly, we observed fewer macrophages in the stroma of α3β1-deficient tumors, some of which were TUNEL-positive indicating enhanced apoptosis. Moreover, we observed reduced mRNA expression within α3β1-deficient tumor cells of the macrophage stimulating cytokine, CSF1, consistent with loss of a tumor cell-derived paracrine signal for recruitment or retention of tumor-associated macrophages. Secondly, α3β1-deficient tumors displayed reduced levels of fibulin-2 in the stroma, and reduced fibulin-2 gene expression within tumor cells, consistent with our previous findings that α3β1 regulates fibulin-2 expression in immortalized mouse keratinocytes *in vitro* (Missan et al., 2014), and in murine neonatal skin and adult wounds *in vivo* (Longmate et al., 2014). We also previously showed that suppression of fibulin-2 caused reduced invasion of transformed keratinocytes *in vitro*, although it did not alter tumor growth *in vivo* (Missan et al., 2014), suggesting that keratinocyte-derived fibulin-2 is dispensable at early stages of tumor growth but may become important at later stages of invasion. Determining the precise roles of fibulin-2 and CSF1 within the TME of the skin tumorigenesis model is an important future direction.

In summary, we have demonstrated that integrin α3β1 is an important regulator of genes that contribute to the keratinocyte secretome, including CSF1 and fibulin-2. This regulation may allow tumor keratinocytes to stimulate the stroma and modulate the cellular and ECM composition of the TME in a way that supports tumor growth. Our model is consistent with

the widely accepted idea that cellular transformation is not sufficient for the development of malignant tumors, and that tumor growth and cancer progression require a supportive TME (Hanahan and Weinberg, 2011). Indeed, many recent studies have focused on non-tumor cell components of the stroma as drivers of malignant progression, and therapeutic targeting of the TME is likely to become increasingly important (Marcucci et al., 2014, Yuan et al., 2016, Zhang et al., 2014). Our findings suggest that targeting α3β1 on some tumor cells may have pleiotropic anti-tumor effects that extend to the TME.

MATERIALS & METHODS

Animal studies

Details of K14CreERT:$\alpha 3^{flx/flx}$ mice and two-step tumorigenesis experiments, performed as described previously (Longmate et al., 2017), are detailed in the Supplementary Materials and Methods. All animal experiments were approved by the Institutional Animal Care and Use Committee of Albany Medical College.

Histology

Excised papillomas were prepared for frozen or paraffin sectioning as described previously (Longmate et al., 2017). Histology and immunostaining are detailed in the Supplementary Materials and Methods.

In situ RNA detection

Single molecule ISH was performed using the RNAScope Fluorescent Multiplex V1 kit (Advanced Cell Diagnostics; Newark, CA) on fresh frozen tissue sections (see above). Sections were fixed in 4% paraformaldehyde, dehydrated, and digested with protease IV for 30 minutes, then incubated for 2 hours, 40°C with probes to detect fibulin-2 (Cat. # 447931) or CSF1 (Cat. #315621-C3) mRNA, followed by wash and amplification steps as per manufacturer's instruction. Sections were co-stained with DAPI, mounted with ProLong Gold antifade mounting media (Molecular Probes; Eugene, OR), and imaged on a Nikon Eclipse 80i microscope with a Photometrics Cool Snap ES camera. Semi-quantitative analysis of puncta within tumor images was performed in a blinded fashion according to Advanced Cell Diagnostics scoring criteria for RNAScope, using a range of 1 (fewest) to 4 (most).

RNA isolation and qPCR

Papillomas or normal skin were excised, flash-frozen in liquid nitrogen and ground into powder using mortar and pestle. Samples were digested with proteinase K, RNA isolated with Trizol, and cDNA generated using iScript Reverse Transcription Supermix (Bio-Rad; Hercules, CA). qPCR for α3 mRNA was performed using iQ SYBR green Supermix (Bio-Rad). Primer sequences for *Itga3*: 5′-CCACAAGCACCAACCACA-3′; 5′-CAGCATCCCTACCATCAACA-3′. The geometric mean of three reference genes (ActB, Ppia, Polr2a; Bio-Rad) was used for normalization. Relative mRNA levels were calculated using the formula [2^−(Ct target gene − Ct reference genes)] and calculated as a fold-change relative to the average value for normal skin.

Mouse keratinocyte (MK) variants

LTAg-immortalized MK cells, p53-null immortalized MK cells (IMKα3+ or IMKα3−), or RasV12-transformed variants of the latter lines (TMKα3+ or TMKα3−) that express or lack α3β1 were derived previously (Iyer et al., 2005, Lamar et al., 2008). Stable GFP expression in TMKα3− cells (gTMKα3−) was achieved through transduction using pHAGE-IRES-GFP lentiviral vector (gift from Dr. John Lamar). MK variants were cultured in MK growth medium as described (Lamar et al., 2008, Longmate et al., 2014, Missan et al., 2014) for not longer than 4 weeks before use. MK lines are tested several times per year for *Mycoplasma* using a PCR-based method (Young et al., 2010), and all studies were conducted within 6 months of latest test date (12–2018).

Apoptosis Assay

Sub-confluent MK cultures were treated for 24 hours with MK growth medium (negative control), MK medium supplemented with 10 μg/ml blasticidin (positive control), or serum-free medium. Floating and attached cells were harvested and processed using the PE Annexin V Apoptosis Detection Kit I (BD Pharmingen; San Diego, CA), then analyzed by flow cytometry on a FACSCanto (BD Biosciences; Bedford, MA).

Cell Proliferation Assay

Triplicate samples of 1×10^3 cells were plated on a 96-well dish in MK growth medium. Phase images were acquired daily on a SpectraMax plate reader (Molecular Devices; San Jose, CA) for 4 days, and cells were counted using Softmax Pro Software (Molecular Devices). Mixed cell experiments were performed in the same manner except that gTMKα3− cells were plated in a 1:1 ratio with either TMKα3+ or TMKα3− cells to total 1×10^3 cells per well, and fluorescent images were acquired to assess gTMKα3− cells.

Mass Spectrometry of MK cell secretome

Duplicate samples of serum-free medium were conditioned for 24 hours by each MK cell variant, passed through a 40 μm cell strainer, then centrifuged for 10 minutes at 2×10^3 g before equal protein was analyzed by MS (Thermo Fisher Center for Multiplexed Proteomics, Harvard Medical School; Boston, MA). MS spectra were searched using the SEQUEST algorithm against a Uniprot composite database derived from the mouse proteome, and peptide spectral matches were filtered to <1% false discovery rate using the target-decoy strategy combined with linear discriminant analysis. Raw summed intensity values were normalized to the geometric mean of the 50 most stable reference proteins. Reference protein stability was determined by calculating a reference gene stability (M-score) using the r package ctrlGene and the geNorm algorithm on raw summed intensity values of all proteins quantified by a minimum of 20 spectral counts (1654 reference candidates) (Vandesompele et al., 2002). Normalized intensity values were used to calculate fold-change in protein abundance in conditioned medium from MKα3+ cells compared with MKα3− cells. The α3β1-dependent secretome was defined by selecting proteins with relative abundance that varied by at least 50% (1.5-fold) and are known or predicted to be secreted using the human and animal secretome and subcellular proteome knowledgebase (MetazSecKB) (Meinken et al., 2015).

Gene Set Enrichment Analysis (GSEA)

GSEA software was downloaded from Broad Institute (Cambridge, MA) (Mootha et al., 2003, Subramanian et al., 2005). To generate a gene set that represents the α3β1-dependent keratinocyte secretome, we used the human homologs corresponding to the 144 mouse proteins that were ≥50% (1.5-fold) higher in MKα3+ cells than in MKα3− cells. To compare tumors to normal skin, gene expression data (Affymetrix Mouse Gene 1.1 ST Array) from wildtype mouse skin and DMBA/TPA two-step tumorigenesis-induced papillomas was downloaded from GEO DataSets (GSE63967) (McCreery et al., 2015). GSEA was performed using the murine α3β1-dependent secretome gene set to compare 9 normal skin samples with 19 papillomas. To perform GSEA of human SCC, RNAseq data from 500 human primary head and neck SCC (harmonized data from TCGA-HNSC) were downloaded and processed using the TCGAbiolinks R/Bioconductor package (Colaprico et al., 2016). TCGA-HNSC data were normalized from read counts using LOESS robust local regression, global-scaling, and full-quantile normalization (Risso et al., 2011). Tumors were grouped by expression of *ITGA3*, then tumors from the highest and lowest 25% (125 samples each) were subjected to GSEA using the human homologs of the α3β1-dependent secretome as the gene set.

Supplementary Material

Refer to Web version on PubMed Central for supplementary material.

ACKNOWLEDGEMENTS

We thank Christina Nickerson (Albany Medical Center Histology Core) for tissue sectioning, Matthew Roos for technical assistance, Drs. John Lamar and Gabrielle Fredman for reagents and valuable advice, and Dr. Susan LaFlamme for critical reading of the manuscript. We thank Thermo Fisher Scientific Center for Multiplexed Proteomics at Harvard Medical School for MS analysis. This research was supported by NIH grants from NIAMS to C. M. DiPersio and L. Van De Water (R01AR063778) and from NCI to C.M. DiPersio (R01CA129637).

Abbreviations:

ECM	extracellular matrix
TME	tumor microenvironment
SCC	squamous cell carcinoma
GSEA	gene set enrichment analysis
K14	keratin-14
4OHT	4-hydroxytamoxifen
MS	mass spectrometry
ISH	*in situ* hybridization
CSF1	colony stimulating factor 1
IL-1α	interleukin-1α

REFERENCES

Abel EL, Angel JM, Kiguchi K, DiGiovanni J. Multi-stage chemical carcinogenesis in mouse skin: fundamentals and applications. Nat Protoc 2009;4(9):1350–62. [PubMed: 19713956]

Colaprico A, Silva TC, Olsen C, Garofano L, Cava C, Garolini D, et al. TCGAbiolinks: an R/Bioconductor package for integrative analysis of TCGA data. Nucleic Acids Res 2016;44(8):e71. [PubMed: 26704973]

Cooper J, Giancotti FG. Integrin Signaling in Cancer: Mechanotransduction, Stemness, Epithelial Plasticity, and Therapeutic Resistance. Cancer Cell 2019;35(3):347–67. [PubMed: 30889378]

Hamidi H, Ivaska J. Every step of the way: integrins in cancer progression and metastasis. Nat Rev Cancer 2018;18(9):533–48. [PubMed: 30002479]

Hanahan D, Weinberg RA. Hallmarks of cancer: the next generation. Cell 2011;144(5):646–74. [PubMed: 21376230]

He Y, Thriene K, Boerries M, Hausser I, Franzke CW, Busch H, et al. Constitutional absence of epithelial integrin alpha3 impacts the composition of the cellular microenvironment of ILNEB keratinocytes. Matrix Biol 2018;74:62–76. [PubMed: 30466509]

Hynes RO. Integrins: bidirectional, allosteric signaling machines. Cell 2002;110(6):673–87. [PubMed: 12297042]

Iyer V, Pumiglia K, DiPersio CM. Alpha3beta1 integrin regulates MMP-9 mRNA stability in immortalized keratinocytes: a novel mechanism of integrin-mediated MMP gene expression. J Cell Sci 2005;118(Pt 6):1185–95. [PubMed: 15728252]

Jones CV, Ricardo SD. Macrophages and CSF-1: implications for development and beyond. Organogenesis 2013;9(4):249–60. [PubMed: 23974218]

Joyce JA, Pollard JW. Microenvironmental regulation of metastasis. Nat Rev Cancer 2009;9(4):239–52. [PubMed: 19279573]

Lamar JM, Pumiglia KM, DiPersio CM. An immortalization-dependent switch in integrin function up-regulates MMP-9 to enhance tumor cell invasion. Cancer Res 2008;68(18):7371–9. [PubMed: 18794124]

Lim YZ, South AP. Tumour-stroma crosstalk in the development of squamous cell carcinoma. Int J Biochem Cell Biol 2014;53:450–8. [PubMed: 24955488]

Longmate WM, Lyons SP, Chittur SV, Pumiglia KM, Van De Water L, DiPersio CM. Suppression of integrin alpha3beta1 by alpha9beta1 in the epidermis controls the paracrine resolution of wound angiogenesis. J Cell Biol 2017;216(5):1473–88. [PubMed: 28416479]

Longmate WM, Lyons SP, DeFreest L, Van De Water L, DiPersio CM. Opposing Roles of Epidermal Integrins alpha3beta1 and alpha9beta1 in Regulation of mTLD/BMP-1-Mediated Laminin-gamma2 Processing during Wound Healing. J Invest Dermatol 2018;138(2):444–51. [PubMed: 28923241]

Longmate WM, Monichan R, Chu ML, Tsuda T, Mahoney MG, DiPersio CM. Reduced fibulin-2 contributes to loss of basement membrane integrity and skin blistering in mice lacking integrin alpha3beta1 in the epidermis. J Invest Dermatol 2014;134(6):1609–17. [PubMed: 24390135]

Marcucci F, Bellone M, Caserta CA, Corti A. Pushing tumor cells towards a malignant phenotype: stimuli from the microenvironment, intercellular communications and alternative roads. Int J Cancer 2014;135(6):1265–76. [PubMed: 24174383]

McCreery MQ, Halliwill KD, Chin D, Delrosario R, Hirst G, Vuong P, et al. Evolution of metastasis revealed by mutational landscapes of chemically induced skin cancers. Nat Med 2015;21(12):1514–20. [PubMed: 26523969]

Meinken J, Walker G, Cooper CR, Min XJ. MetazSecKB: the human and animal secretome and subcellular proteome knowledgebase. Database (Oxford) 2015;2015.

Missan DS, Chittur SV, DiPersio CM. Regulation of fibulin-2 gene expression by integrin alpha3beta1 contributes to the invasive phenotype of transformed keratinocytes. J Invest Dermatol 2014;134(9):2418–27. [PubMed: 24694902]

Mitchell K, Svenson KB, Longmate WM, Gkirtzimanaki K, Sadej R, Wang X, et al. Suppression of integrin alpha3beta1 in breast cancer cells reduces cyclooxygenase-2 gene expression and inhibits

tumorigenesis, invasion, and cross-talk to endothelial cells. Cancer Res 2010;70(15):6359–67. [PubMed: 20631072]

Mitchell K, Szekeres C, Milano V, Svenson KB, Nilsen-Hamilton M, Kreidberg JA, et al. Alpha3beta1 integrin in epidermis promotes wound angiogenesis and keratinocyte-to-endothelial-cell crosstalk through the induction of MRP3. J Cell Sci 2009;122(Pt 11):1778–87. [PubMed: 19435806]

Mootha VK, Lindgren CM, Eriksson KF, Subramanian A, Sihag S, Lehar J, et al. PGC-1alpha-responsive genes involved in oxidative phosphorylation are coordinately downregulated in human diabetes. Nat Genet 2003;34(3):267–73. [PubMed: 12808457]

Obaya AJ, Rua S, Moncada-Pazos A, Cal S. The dual role of fibulins in tumorigenesis. Cancer Lett 2012;325(2):132–8. [PubMed: 22781395]

Perez-Riverol Y, Csordas A, Bai J, Bernal-Llinares M, Hewapathirana S, Kundu DJ, et al. The PRIDE database and related tools and resources in 2019: improving support for quantification data. Nucleic Acids Res 2019;47(D1):D442–D450. [PubMed: 30395289]

Ratushny V, Gober MD, Hick R, Ridky TW, Seykora JT. From keratinocyte to cancer: the pathogenesis and modeling of cutaneous squamous cell carcinoma. J Clin Invest 2012;122(2):464–72. [PubMed: 22293185]

Risso D, Schwartz K, Sherlock G, Dudoit S. GC-content normalization for RNA-Seq data. BMC Bioinformatics 2011;12:480. [PubMed: 22177264]

Sachs N, Secades P, van Hulst L, Kreft M, Song JY, Sonnenberg A. Loss of integrin alpha3 prevents skin tumor formation by promoting epidermal turnover and depletion of slow-cycling cells. Proc Natl Acad Sci U S A 2012;109(52):21468–73. [PubMed: 23236172]

Subramanian A, Tamayo P, Mootha VK, Mukherjee S, Ebert BL, Gillette MA, et al. Gene set enrichment analysis: a knowledge-based approach for interpreting genome-wide expression profiles. Proc Natl Acad Sci U S A 2005;102(43):15545–50. [PubMed: 16199517]

Vandesompele J, De Preter K, Pattyn F, Poppe B, Van Roy N, De Paepe A, et al. Accurate normalization of real-time quantitative RT-PCR data by geometric averaging of multiple internal control genes. Genome Biol 2002;3(7):RESEARCH0034. [PubMed: 12184808]

Vasioukhin V, Degenstein L, Wise B, Fuchs E. The magical touch: genome targeting in epidermal stem cells induced by tamoxifen application to mouse skin. Proc Natl Acad Sci U S A 1999;96(15):8551–6. [PubMed: 10411913]

Wang F, Flanagan J, Su N, Wang LC, Bui S, Nielson A, et al. RNAscope: a novel in situ RNA analysis platform for formalin-fixed, paraffin-embedded tissues. J Mol Diagn 2012;14(1):22–9. [PubMed: 22166544]

Wettersten HI, Weis SM, Pathria P, von Schalscha T, Minami T, Varner JA, et al. Arming tumor-associated macrophages to reverse epithelial cancer progression. Cancer Res 2019.

Yang X, Li Y, Zou L, Zhu Z. Role of Exosomes in Crosstalk Between Cancer-Associated Fibroblasts and Cancer Cells. Front Oncol 2019;9:356. [PubMed: 31131261]

Young L, Sung J, Stacey G, Masters JR. Detection of Mycoplasma in cell cultures. Nat Protoc 2010;5(5):929–34. [PubMed: 20431538]

Yuan Y, Jiang YC, Sun CK, Chen QM. Role of the tumor microenvironment in tumor progression and the clinical applications (Review). Oncol Rep 2016;35(5):2499–515. [PubMed: 26986034]

Zhang S, Mercado-Uribe I, Liu J. Tumor stroma and differentiated cancer cells can be originated directly from polyploid giant cancer cells induced by paclitaxel. Int J Cancer 2014;134(3):508–18. [PubMed: 23754740]

Zheng R, Longmate WM, DeFreest L, Varney S, Wu L, DiPersio CM, et al. Keratinocyte Integrin alpha3beta1 Promotes Secretion of IL-1alpha to Effect Paracrine Regulation of Fibroblast Gene Expression and Differentiation. J Invest Dermatol 2019.

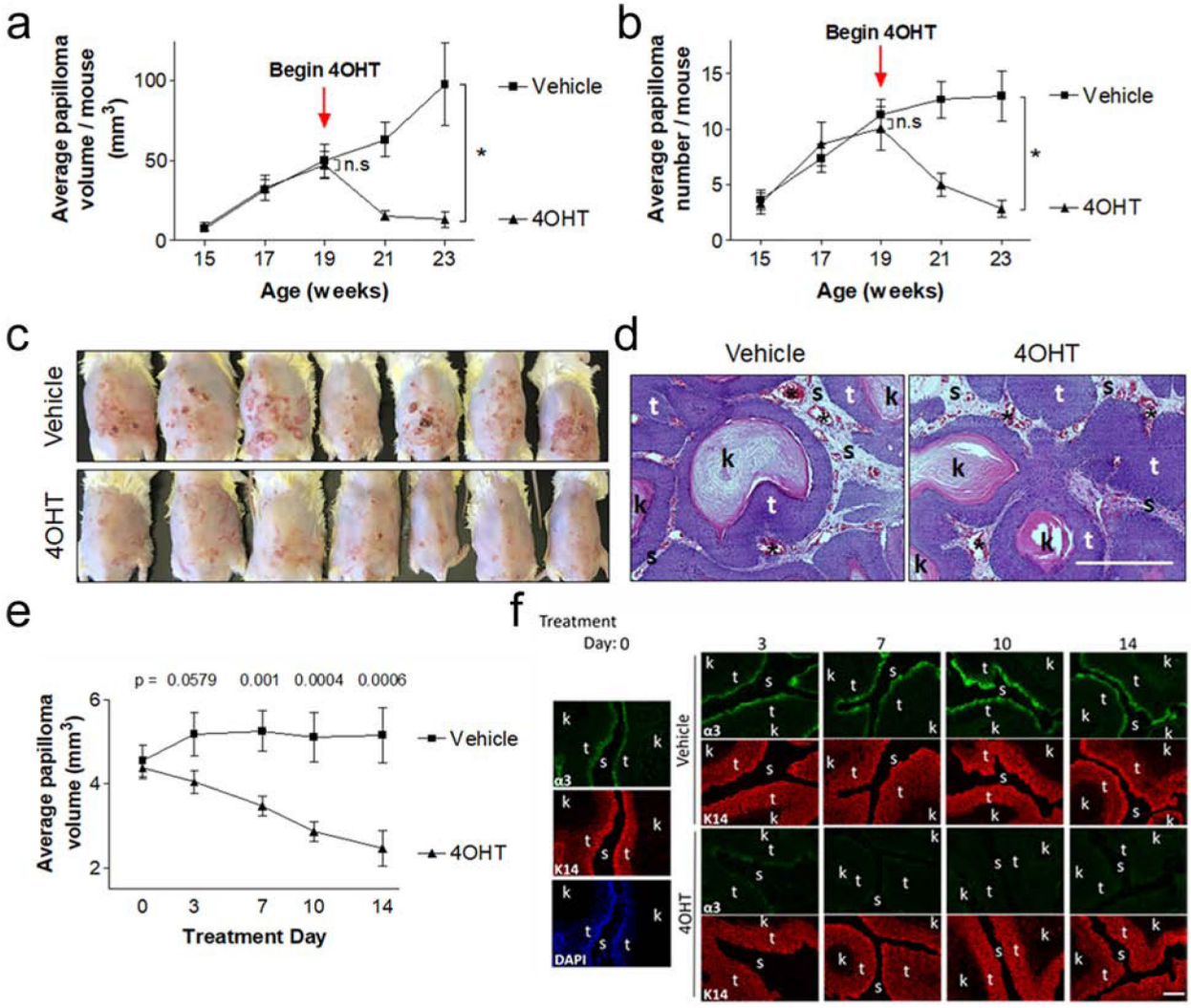

Figure 1.

4OHT-treated tumors in K14CreERT:$\alpha 3^{flx/flx}$ mice regress with coincident α3β1 loss. Following two-step tumorigenesis, papillomas were treated with 4OHT or vehicle starting at 19 weeks old (Treatment Day 0). (a,b) Graphs, average tumor (a) volume and (b) number per mouse; n=7 mice/group. (c) Backs of mice, 23-weeks old. (d) H&E of paraffin tumor sections; scale bar, 500 μm. (e,f) Tumors were measured and harvested at 3, 7, 10 or 14 days after 4OHT treatment. (e) Graph, average tumor volume; n≥45 papillomas per group, per timepoint. (f) Tumor cryosections co-stained with anti-K14, anti-α3, and DAPI (day 0); n≥13 tumors per group, per timepoint; scale bar, 100 μm. *t*, tumor cells; *s*, stroma; *k*, keratinized region; *, blood vessels. (a,b,e) Mean +/− s.e.m.; two-tailed t-tests; *P<0.05; *ns*, not significant.

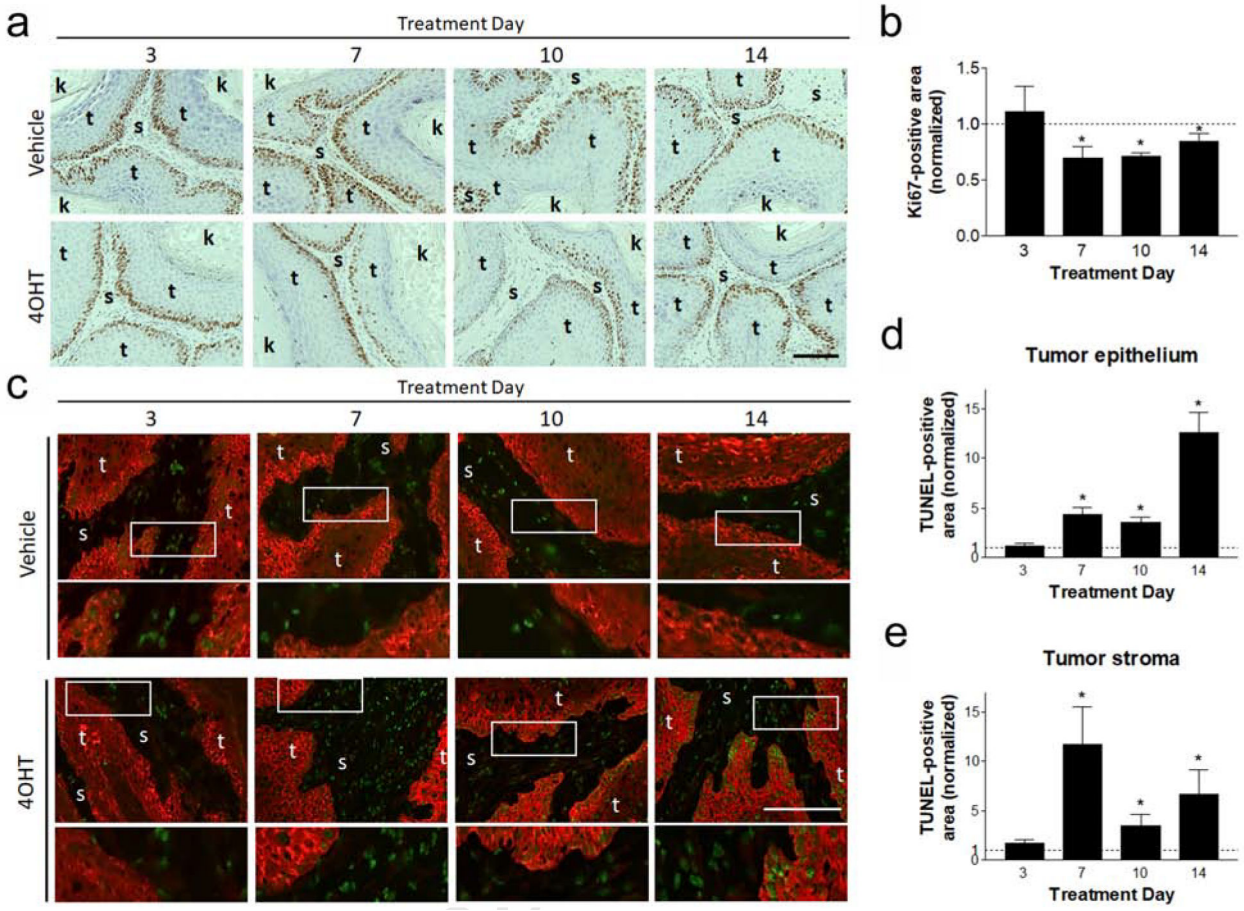

Figure 2.

Regression of α3β1-deficient tumors is accompanied by reduced cell proliferation and increased apoptosis. K14CreERT:$\alpha 3^{flx/flx}$ mice were subjected to two-step tumorigenesis, then treated with 4OHT or vehicle, as in Figure 1e. (a) Paraffin-sectioned tumors stained with anti-Ki67 and hematoxylin counterstain. (b) Graph shows % Ki67-positive area relative to total papilloma area. (c) Tumor cryosections stained with anti-K14 (red) and TUNEL (green); indicated regions enlarged 2.3X below each panel. (d,e) Graphs, % TUNEL+ area relative to (d) epithelial area or (e) stromal area. (a,c) *t*, tumor cells; *s*, stroma; *k*, keratinized region; scale bars, 100 μm. (b,d,e) 4OHT-treated tumor data are normalized to vehicle-treated papillomas (dotted line); n≥10 tumors per treatment group, per timepoint. Data are mean +/− s.e.m.; two-tailed t-tests; *P<0.05.

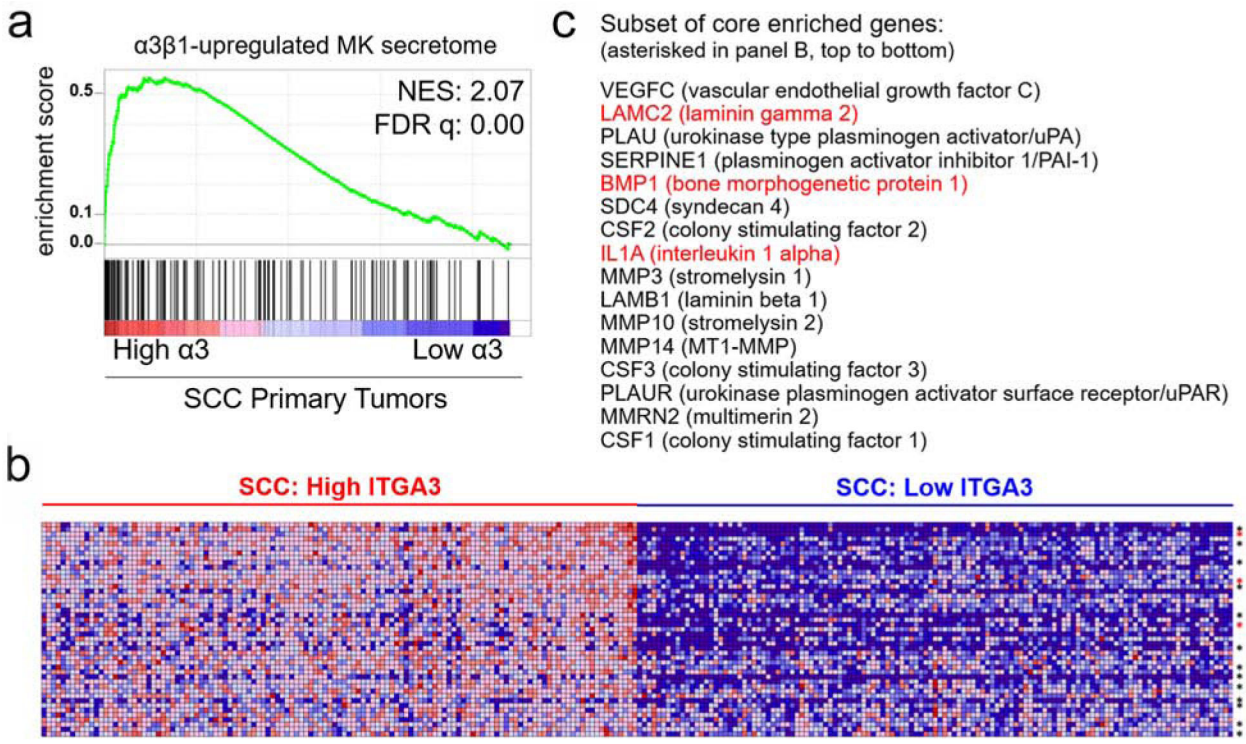

Figure 3.

GSEA of human SCC with high vs. low *ITGA3* gene expression shows enrichment of expression of genes that encode the upregulated α3β1-dependent MK secretome. (a) The α3β1-dependent MK secretome gene set was defined as proteins measured by quantitative MS that showed upregulated secretion in MKα3+ relative to MKα3− cells. GSEA was performed on RNA expression data from high and low *ITGA3*-expressing SCCs using the α3β1-dependent secretome as the gene set (NES = 2.07, FDR q-value = 0.00). (b) Expression heatmap of genes corresponding to core enrichment of α3β1-dependent MK secretome within high and low *ITGA3*-expressing SCCs. (c) Subset of genes (asterisked in panel b) from the α3β1-dependent secretome that showed core enrichment; red text indicates those we linked previously to α3β1-dependent MK functions (see text).

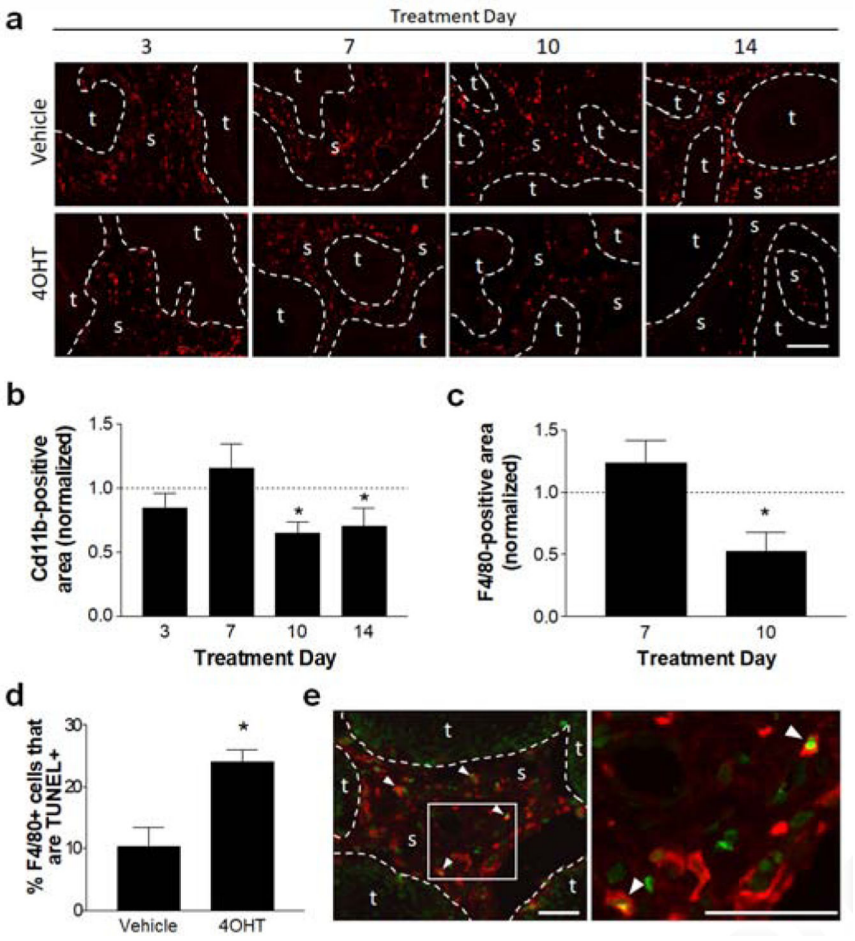

Figure 4.

Regressed α3β1-deficient tumors have fewer macrophages. K14CreERT:$\alpha 3^{flx/flx}$ mice were subjected to two-step tumorigenesis then treated with 4OHT or vehicle, as in Figure 1e. (a) Cryosections stained with anti-CD11b (red); *t*, tumor cells; *s*, stroma; *dashed line*, tumor-stroma boundary; scale bar, 200 μm. (b, c) Graphs show (b) CD11b+ area or (c) F4/80+ area relative to total area in 4OHT-treated tumors, normalized to vehicle (*dotted line*). (d) % F4/80-positive cells that are TUNEL-positive at treatment day 7. (b-d) n≥8 papillomas per group, per timepoint. Data are mean +/− s.e.m.; two-tailed t-tests; *P<0.05. (e) Representative tumor 7-days post-4OHT treatment, co-stained with F4/80 (red) and TUNEL (green); box in left panel is enlarged in right panel. *Arrowheads*, TUNEL-positive macrophages; *t*, tumor cells; *s*, stroma; *dashed line*, tumor-stroma boundary; scale bars, 50 μm.

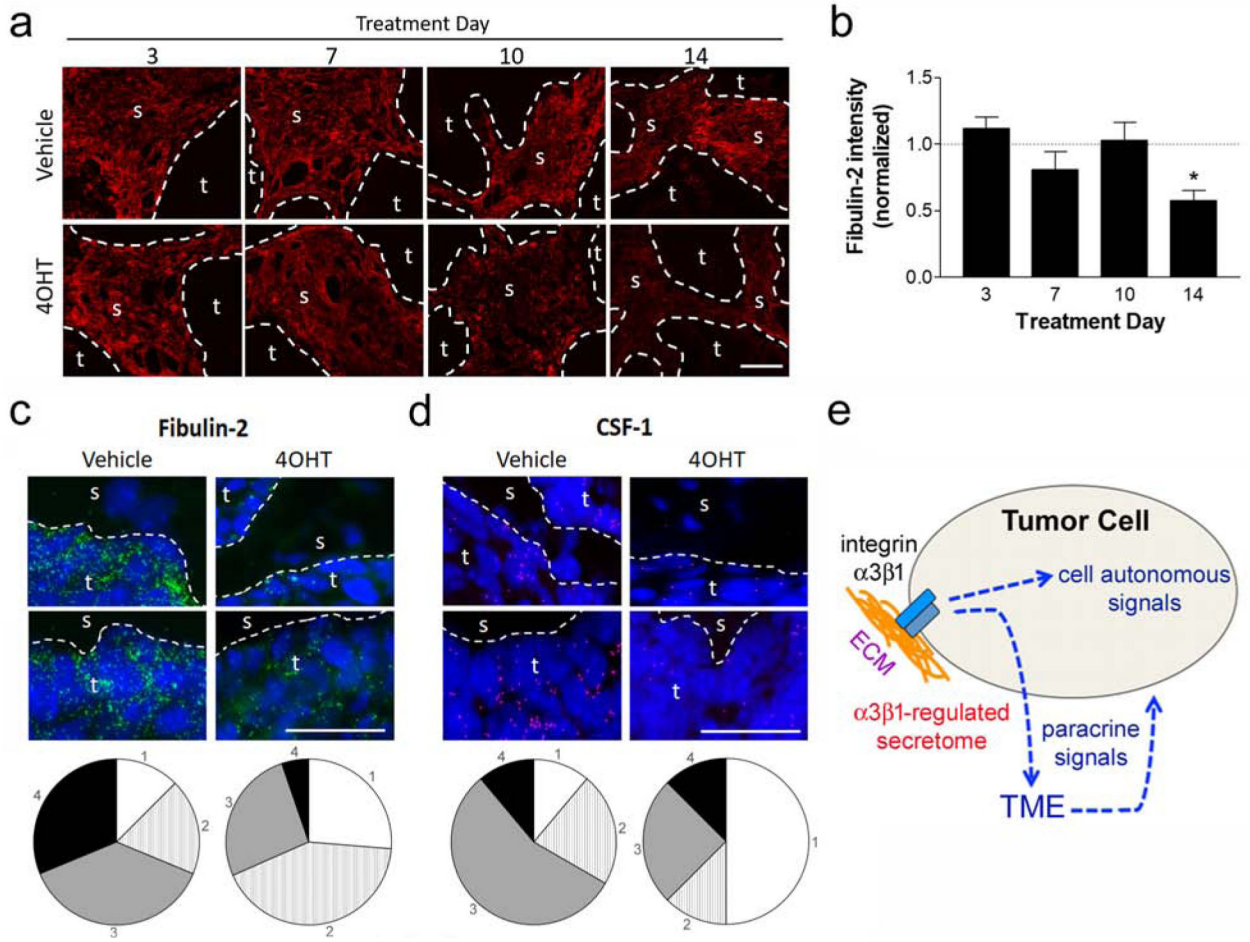

Figure 5.

Fibulin-2 and CSF1 are reduced in α3β1-deficient tumors. K14CreERT:$\alpha 3^{flx/flx}$ mice were subjected to two-step tumorigenesis then treated with 4OHT or vehicle, as in Figure 1e. (a) Cryosections stained with anti-fibulin-2. *t*, tumor cells; *s*, stroma; *dashed line*, tumor-stroma boundary; scale bar, 100 μm. (b) Quantified fibulin-2 MFI in 4OHT-treated papillomas, normalized to vehicle (*dotted line*); n≥13 papillomas per group, per timepoint. Mean +/− s.e.m.; two-tailed t-tests; *P<0.05. (c,d) ISH of cryosections from treatment day 14. Representative images for (c) fibulin-2 mRNA (green) or (d) CSF1 mRNA (purple); DAPI (blue) marks nuclei; scale bar, 25 μm. Pie charts, blind-score distribution (n≥8). Image scores: (c) Vehicle, #4; 4OHT, #2; (d) Vehicle, #3; 4OHT, #1. (e) Model: α3β1 regulates secreted factors from tumor cells that promote a pro-tumoral TME.